Unsupervised Eye Blink Artifact Denoising of EEG Data with Modified Multiscale Sample Entropy, Kurtosis, and Wavelet-ICA

Ruhi Mahajan, *Student Member, IEEE*, and Bashir I. Morshed, *Member, IEEE*

***Abstract*—Brain activities commonly recorded using the electroencephalogram (EEG) are contaminated with ocular artifacts. These activities can be suppressed using a robust independent component analysis (ICA) tool, but its efficiency relies on manual intervention to accurately identify the independent artifactual components. In this paper, we present a new unsupervised, robust, and computationally fast statistical algorithm that uses modified multiscale sample entropy (mMSE) and Kurtosis to automatically identify the independent eye blink artifactual components, and subsequently denoise these components using biorthogonal wavelet decomposition. A 95% two-sided confidence interval of the mean is used to determine the threshold for Kurtosis and mMSE to identify the blink related components in the ICA decomposed data. The algorithm preserves the persistent neural activity in the independent components and removes only the artifactual activity. Results have shown improved performance in the reconstructed EEG signals using the proposed unsupervised algorithm in terms of mutual information, correlation coefficient, and spectral coherence in comparison with conventional zeroing-ICA and wavelet enhanced ICA artifact removal techniques. The algorithm achieves an average sensitivity of 90% and an average specificity of 98%, with average execution time for the datasets ($N = 7$) of 0.06 s ($\mathrm{SD} = 0.021$) compared to the conventional wICA requiring 0.1078 s ($\mathrm{SD} = 0.004$). The proposed algorithm neither requires manual identification for artifactual components nor additional electrooculographic channel. The algorithm was tested for 12 channels, but might be useful for dense EEG systems.**

***Index Terms*—Artifact removal, biorthogonal wavelet, electroencephalogram (EEG), independent component analysis (ICA), kurtosis, modified multiscale sample entropy (mMSE).**

I. Introduction

NEURONAL activities along the cortex can be recorded noninvasively using scalp electroencephalogram (EEG). EEG recordings can be related to certain mental states, audio-visual cues, attention, cognitive loads, and various disorders. This is of recent interest to monitor patients in practical settings with complex neurological disorders including epilepsy, attention deficit hyperactivity disorder (ADHD), autism spectrum disorder, posttraumatic stress disorder, and Alzheimer's disease. In the practical settings, EEG recordings are often affected by the extrinsic artifacts due to power line interferences and intrinsic physiological artifacts due to ocular activities (eye blink, saccades, and fixations), muscle activity, and cardiac activity. Power line interferences can be filtered by using high Q notch filter. The subject may also be asked to avoid the excessive movements to reduce muscle related artifacts. However, it is challenging for the subjects to avoid their ocular activities. Specifically, eye blinks are the common biological phenomenon with average blink duration between 100–400 milliseconds. It is very crucial therefore to remove the blink related activities as these high amplitude signals (can reach up to 800 μV) might mislead the analysis [1]. One of the common practices to remove ocular artifacts is to use regression-based methods [2]. But, these methods need the recordings of the electrooculographic channel (EOG) [3]. It is also difficult to design an optimal regression model suitable for all types of artifacts. Another conventional method to remove the eye blinks is using the linear filters with the cut-off frequency with respect to artifact range [4]. However, the time-domain or frequency domain filtering can give substantial loss of the cerebral activity because of spectral overlap between neurological and artifactual events [5]. There is also consensus among researchers for using statistical techniques like independent component analysis (ICA) [6], principal component analysis (PCA) [7], multiresolution denoising [8]–[10], and wavelet with higher order statistics [11] for artifact correction. Among these methods, ICA is perceived to be a very robust method for ocular artifact removal, but its procedure requires manually identifying the artifactual independent components. Though Kurtosis, data improbability, linear trends, and spectral temporal maps [12] are proposed for component identification, most of these methods either need the recording of an additional EOG signal for reference or expertise intervention to mark the noisy components, hence making it a time consuming and arduous process.

Higher order statistics such as modified multiscale sample entropy (mMSE) along with Kurtosis to identify the eye blink distributions in EEG has been mostly unexplored. This study indicates that mMSE is a strong identifier of the blink related artifactual components, and incorporation of Kurtosis further strengthens the identification accuracy. Following up our previous study [13], this paper proposes an unsupervised fully automatic statistical threshold based eye blink artifact removal method using mMSE and Kurtosis to identify the artifactual blink components and multiresolution wavelet analysis to denoise these components. The algorithm thresholds only the

Manuscript received January 15, 2014; revised April 23, 2014 and June 17, 2014; accepted 20, 2014. Date of publication June 25, 2014; date of current version December 30, 2014. This work was partially supported by Strengthening Communities Initiative (SCI) Capacity Building Grant, 2012.

R. Mahajan and B. I. Morshed are with the Department of Electrical and Computer Engineering, The University of Memphis, Memphis, TN 3815 USA (e-mail: rmhajan1@memphis.edu; bmorshed@memphis.edu).

Color versions of one or more of the figures in this paper are available online at http://ieeexplore.ieee.org.

Digital Object Identifier 10.1109/JBHI.2014.2333010

wavelet coefficients corresponding to the artifactual activity to zero in the wavelet decomposition, retaining the neural activities persistent in the blink ICs intact, while suppressing the blink activities. The following sections present this proposed method with pilot data for comparative evaluation.

II. ICA, mMSE, and Kurtosis

This section describes the extended-infomax ICA decomposition method to obtain the statistically independent components (IC) and the markers for recognizing the artifactual ICs.

A. ICA for IC decomposition

ICA is the widely accepted tool for decomposing the multivariate EEG data into its statistical independent, nonGaussian components. The ICA models are applied for EEG analysis with underlying plausible assumptions:

1) The cerebral and artifactual sources are linearly mixed and are statistically independent.
2) The number of observed signals, *S*, are greater than or equal to the number of ICs, u.
3) Propagation delays through the mixing medium (i.e., brain, scalp etc.) are negligible.

The linear ICA model for the observed EEG sources *S* is expressed mathematically as

$$X = A \times S \tag{1}$$

where *X* is the linear mixture of sources, *A* is the unknown mixing matrix [14]–[16]. In this study, we have used extended-Infomax ICA algorithm to calculate the unmixing matrix, *W* so that the components, *u* are as independent as possible and we get the best approximation of *S* as

$$u = W \times X \approx S; \quad W = A^{-1}. \tag{2}$$

The extended-infomax ICA method, an extension of the Infomax decomposition [17] separates the sub-Gaussian and super-Gaussian distribution of the sources by minimizing the mutual information between the components and maximizing their joint entropy. The Infomax algorithm in this paper is implemented using the *runica* function of the EEGLAB toolbox (MATLAB, CA, US) with its default settings.

B. mMSE as an Artifact Marker

The concept of using entropy in terms of wavelet entropy, Shannon's entropy, Renyi's entropy, and sample entropy has been already found useful in identifying the artifact related ICs [18]. Recently, it has been revealed by Bosl *et al*. that MSE gives much more information about the regularity of the EEG time-series than the aforementioned entropies of the single scale [19]. Thus, this study explores the use of mMSE to identify eye blinks in EEG recordings.

The intuition that mMSE can identify the artifact related components lies in the fact that the eye-blinks are concentrated in the small temporal intervals with high probabilities and low entropy. In other words, the expected value of mMSE for the blink related component is low because its pattern is more regular and predictable in comparison with neural activity. So, mMSE could be a good statistical measure to recognize ocular activities.

In this paper, mMSE is implemented by first coarse graining each IC for multiple scales and then computing the sample entropy for each scale. As the EEG recordings used in this study have 10 000 data points, we have used a fixed scale factor, $\tau = 20$, as the minimum length of the grained series, which in this case will contain 500 data points is sufficient for the information we seek. The coarse graining of each IC of the EEG data is computed by averaging the successive data points of the series in nonoverlapping window as

$$y_j^{(\tau)} = \frac{1}{\tau} \sum_{i=(j-1)\tau+1}^{j\tau} u_i; \quad 1 \le j \le {}^{N}\!/_{\tau} \tag{3}$$

$y_j^{(\tau)}$ represents the coarse grained series, τ is scale factor, u represents the IC time-series, and N is the total data points in the original series [20]. The length of each coarse-grained series is limited to N/τ.

The MSE for each grained series $y_j^{(20)}$ is then computed using (4) as explained in [21]:

$$\mathrm{mMSE}(m, r) = \log\left(\frac{{B_r}^m}{{A_r}^m}\right) \tag{4}$$

where maximum length of epochs for matching templates, $m = 2$ and tolerance, $r = 0.2 \times \mathrm{SD}$; SD is the standard deviation of the data vectors. B and A are the counters to track the m and (m + 1) template matches within the tolerance value *r*, respectively. As the entropy for the blink related artifacts is expected to be low, we can use the mMSE to detect the artifact related components with low entropy values. The threshold for the automatic identification algorithm to find the noisy components is explained in the Section III.

C. Kurtosis as an Artifact Marker

Kurtosis is the fourth-order cumulant to measure the peaked distributions of the random variables and is mathematically computed using the following equations:

$$k = m_4 - 3m_2^2 \tag{5}$$

$$m_n = E\left\{(x - m_1)^n\right\} \tag{6}$$

where m_n, m_1, and *E* are the nth order central moment of the variable, mean, and the expectation function, respectively [16]. In the practical settings of continuous EEG recordings, the components with cardiac and eye blink activities have typically peak distributions with highly positive Kurtosis, whereas noise induced by line currents and loose electrode connections have flat distribution with negative Kurtosis [12]. So, measuring Kurtosis of the ICA decomposed EEG data, we can find the components related to eye blink activities. In this paper, an inbuilt MATLAB function *kurtosis* is used to compute the Kurtosis for each IC.

III. Proposed Unsupervised Automatic Algorithm

This section describes the data acquisition protocol, a fully automatic algorithm to identify the artifacts, and the denoising

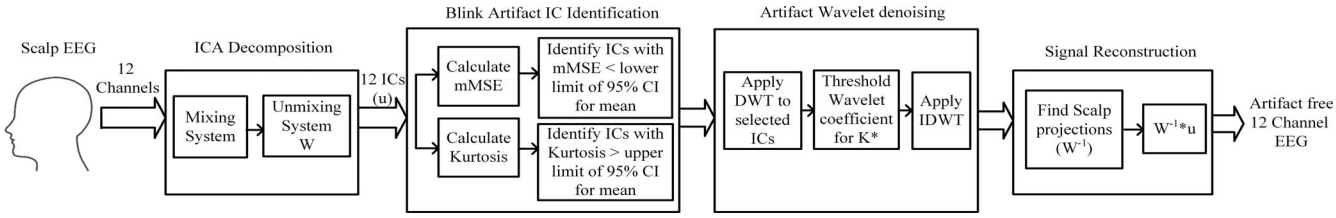

Fig. 1. Block diagram of the proposed eye blink artifact removing algorithm [K^* is calculated using (9) as discussed in the Section III].

procedure to remove the artifact related components. The block diagram of the proposed algorithm is given in Fig. 1.

A. Data Acquisition

A wireless 14-channel referential montage EPOC headset (Emotiv, Eveleigh, NSW, Australia) is used to continuously record the brain activities from the subjects at the sampling rate of 128 sps. The headset has bandwidth of 0.2–45 Hz and digital notch filters to ensure elimination of power line interferences. Data is collected from four subjects (two males and two females) based on the International 10–20 electrode locations at AF3, AF4, F3, F4, F7, F8, FC5, FC6, P7, P8, T7, T8, O1, and O2. The data acquisition has been conducted in an enclosed room with dim light for 1 min 45 s. As per the protocol, at the beginning of the recording session, the subject is asked to close the eyes for 30 s, then open the eyes and blink nine times with a 5-s hiatus. At the end of the session, the subject is again instructed to close eyes for 30 s. The experiment is repeated twice with all the subjects except one subject, resulting in seven datasets to evaluate the proposed blink artifact removal algorithm. The EEG recordings from the subjects in this paper are labeled as Dataset *X* (where $X = 1 \ldots 7$). Because of poor recording quality in FC5 and FC6 channels from Subject 1 (due to loose electrode contacts), these channels were discarded. For uniform analysis, only the best 12-channel recordings were selected from all datasets (discarded channels: Subject 2: T8, F4; Subject 3: F7, T7; and Subject 4: P7, P8). Discarding poor recordings is not expected to alter performance comparison.

B. Procedure for Identifying the Artifactual ICs

In the proposed algorithm, after ICA decomposition of the EEG data, mMSE is computed for all the ICs. As blink artifacts are notable outlier data representing the typical transient events, they can be detected using thresholds after normalized distribution ($\mathrm{Mean} = 0$ and Standard Deviation, $\mathrm{SD} = 1$) of the data [22]. In the current study, the sample size of the ICs ($N = 12$) is small, so instead of classical threshold with 95% confidence interval (CI) for normalized Z-distribution, we have used two-sided 95% CI of the mean for Student's t-distribution to detect the blink artifact ICs. As explained previously, the expected value of mMSE for the blink related artifactual IC is less in comparison with neural activity related IC thus, the proposed fully automatic algorithm uses the lower limit of the 95% CI of the mean for thresholding the IC based on the mMSE. All the ICs with their entropy values higher than the threshold are expected to be belonging to the cerebral signal; while other ICs are marked for wavelet correction. The lower limit of 95% CI of the mean is calculated as

$$\text{Lower limit} = \bar{x} - \frac{s}{\sqrt{N}} \times t_{N-1} \tag{7}$$

where $\bar{x}$ is the sample mean, s is the sample standard deviation, and (*N*-1) is the degrees of freedom. At 95% significance level, $\alpha = 0.05$ and $t_{n-1} = 2.201$ for two-tailed test with 11 degrees of freedom.

To enhance the efficacy of the algorithm, Kurtosis is also used to determine eye blink activity distributions in the IC signal. Kurtosis is zero for Gaussian distribution, positive for the peaked activities (which mimics eye blink signal) and negative for the flat distributions. So, in this study, the upper bound of the 95% CI of the mean [calculated using (8)] is used as the threshold.

$$\text{Upper limit} = \bar{x} + \frac{s}{\sqrt{N}} \times t_{N-1}. \tag{8}$$

All the ICs having Kurtosis higher than the upper limit of CI are supposed to be blink artifacts and are marked for denoising. The calculated statistics: mean, standard deviation (SD), and standard error of the mean (SEM) for all the datasets with their 95% CI of the mean threshold are tabulated in Table I. Thresholds for the mMSE (0.890) and Kurtosis (29.76) for the Dataset 1 are marked with the dotted lines in the Fig. 2. All the components falling below the threshold for mMSE and above threshold for Kurtosis are marked as eye blink artifact components and are further processed for wavelet denoising. Similarly, on the basis of the thresholds computed in the Table I, the components selected for denoising are marked with the sign + in the Fig. 3.

Most of the blink artifact ICs are identified itself by the mMSE but the fourth-order cumulant Kurtosis offers an additional advantage to the detection method by finding the super Gaussian and subGaussian artifact distribution in the ICs.

C. Procedure for Denoising the Artifactual ICs

Once the artifactual ICs are identified, they are processed for artifact suppression. It has been propounded by Castellanos *et al.* [23] that the ICs with artifactual activities should not be simply replaced with zero as they might have the leaked neural signal in it and discarding the entire component will lead to loss of meaningful data. So, in the proposed method, instead of replacing the entire component with zero, we denoise only the contaminated components with biorthogonal wavelets. It differs from this conventional wavelet enhanced ICA (wICA)

TABLE I
COMPUTED STATISTICS FOR THE 12 ICS OF EACH EEG DATASET

Dataset	Statistical Measures	mMSE	Kurtosis
1	*SD*	0.534	19.99
	Mean	1.229	17.06
	SEM	0.154	5.771
	Threshold (95% CI)	**0.890**	**29.76**
2	*SD*	0.562	7.034
	Mean	1.549	7.361
	SEM	0.162	2.031
	Threshold (95% CI)	**1.191**	**11.83**
3	*SD*	0.408	13.55
	Mean	0.987	14.47
	SEM	0.118	3.910
	Threshold (95% CI)	**0.728**	**23.08**
4	*SD*	0.405	17.41
	Mean	1.069	16.92
	SEM	0.117	5.025
	Threshold (95% CI)	**0.812**	**27.98**
5	*SD*	0.427	10.49
	Mean	1.379	10.54
	SEM	0.123	3.028
	Threshold (95% CI)	**1.108**	**17.20**
6	*SD*	0.430	18.31
	Mean	1.342	11.52
	SEM	0.124	5.286
	Threshold (95% CI)	**1.069**	**23.16**
7	*SD*	0.221	13.43
	Mean	1.409	11.03
	SEM	0.064	3.878
	Threshold (95% CI)	**1.269**	**19.56**

Threshold (in bold) mentioned for the mMSE and Kurtosis is the lower bound value and upper bound value of 95% CI for the mean, respectively. The two- tailed t critical for $\alpha = 0.05$ with 11 degrees of freedom is 2.201.

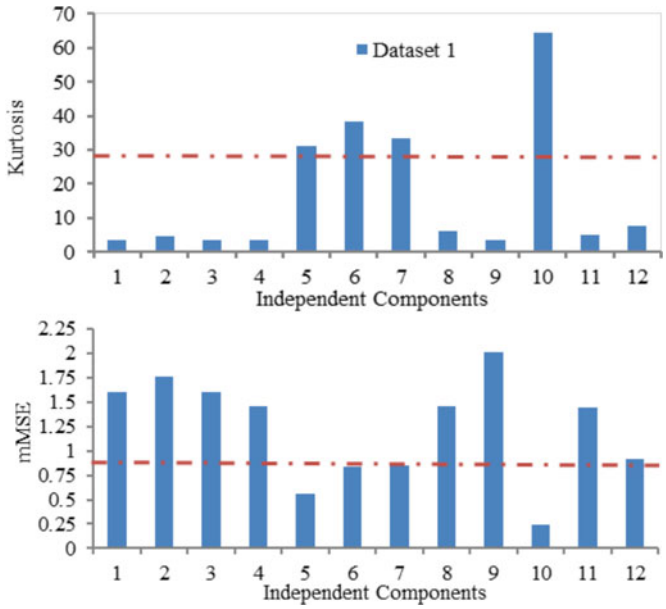

Fig. 2. Kurtosis and mMSE plots with respect to 12 ICs for the Dataset 1. Dotted Line is on the threshold calculated by 95% CI for the mean for both markers. Components 5, 6, 7, and 10 are marked as blink related artifact ICs.

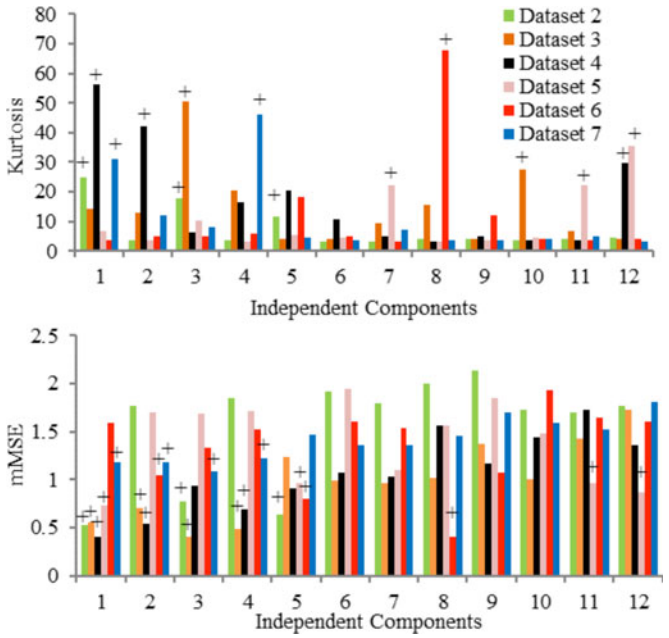

Fig. 3. Kurtosis and mMSE plots with respect to 12 ICs for Dataset 2 to 7. ICs identified as artifacts are marked with + in each plot.

analysis method as wavelet correction is not done unnecessarily on all the ICs. The components which are identified as artifacts are only decomposed with wavelet transform which saves the computation time and complexity. Discrete wavelet transform (DWT), a fast, nonredundant transform performs better on the already digitally sampled data (with finite duration) in contrast with Continuous Wavelet Transform [24], [25], so in this study multiresolution based DWT decomposition is employed. Occurrence of blink artifact in the IC is significantly detected at fourth-level of decomposition with Biorthogonal mother wavelet *bior 4.4* (MATLAB function) [26]. The step-wise attenuation procedure is given below:

1) Evaluate the DWT decomposition of the identified eye blink artifact IC.
2) If the wavelet coefficient exceeds the value *K* [calculated using (9)], threshold them to zero:

$$K = \sqrt{2\text{logN}}\,\sigma \tag{9}$$

where

$$\sigma^2 = \text{median}\ (|W(j,k)|/0.6745) \tag{10}$$

estimates the magnitude of the neuronal wide band signal with constant 0.6745 accounting for the Gaussian noise, $|W(j, k)|$ is the absolute value of the wavelet coefficients and N is the length of the data to be processed. (The threshold for wavelet denoising used above is robust and gives good performance with ocular artifacts as discussed in [23] and explained in [27]–[30]).

3) Compute the Inverse Discrete Wavelet Transform (IDWT) of the thresholded coefficients and recompose the components with neuronal activity only.

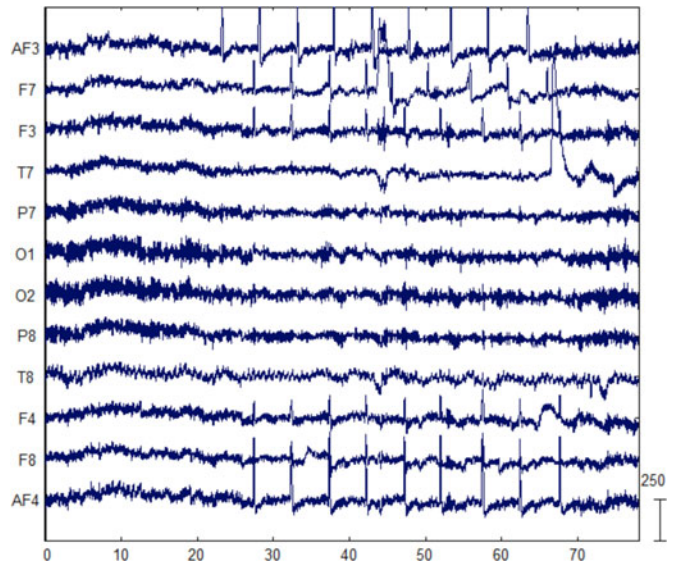

Fig. 4. Raw 12-channel EEG data from the Dataset 1. *X*-axis is time in seconds and *Y*-axis is amplitude in microvolts.

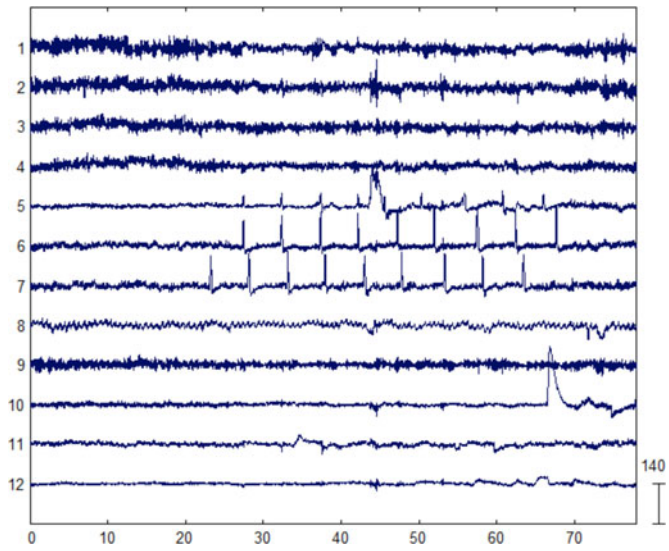

Fig. 5. IC plots of the ICA decomposed EEG data of Dataset 1. ICs 5, 6, 7, and 10 exhibits the properties of eye blink artifactual components.

4) Reconstruct the blink artifact free 12-channel EEG signal by multiplying scalp projections (W^{-1}, obtained from the ICA decomposition) with the inverse transformed wavelet coefficients.

The algorithm has been realized in MATLAB (MathWorks, CA, US). The algorithm being fully automatic does not require any manual visual inspection for the detection and suppression of the artifacts.

IV. Results

The 12-channel preprocessed EEG signals of the Dataset 1 for 78 s duration is plotted using MATLAB in Fig. 4. The eye blinks can be conspicuously seen in the prefrontal cortex region AF3, F7, F3, F4, F8, and AF4. This was also verified with the spectral and temporal plots in EEGLAB software (not included in the paper due to space constraint). After the ICA decomposition of the data, 12 ICs are obtained as plotted in the Fig. 5. The proposed algorithm is applied to all the ICs, then using the markers: mMSE and Kurtosis, the eye blink related ICs are identified and suppressed using the Wavelet transformation. The blink artifact clean EEG data of the same dataset is plotted in Fig. 6. It can be observed in Fig. 6 that the blink related amplitude for frontal lobe electrode locations is significantly attenuated in contrast to Fig. 4.

For comparison with the proposed technique, the ICs obtained from the ICA decomposition are also visually classified as the eye blink artifact ICs and other ICs based on their the scalp map projection, component activity and the power spectrum plots in EEGLAB. The spectral and temporal properties of the components are evaluated as per the guidelines in EEGLAB tutorial [31]. A comparison plot of the proposed method with Zeroing- ICA method is shown in Fig. 7 for a section of EEG data from Dataset 1 AF3 location. It is evident from the plot that manual zeroing-ICA corrected data is deviated more from the raw signal than the proposed method. The performance of the unsupervised proposed algorithm is also statistically analyzed by calculating True Positive (IC marked for rejection both by the algorithm and visual inspection check), False Positive (IC marked by the algorithm but not with the visual inspection), True Negative (IC marked neither by the algorithm nor with the visual inspection), and False Negative (IC not marked with the algorithm but with the visual inspection). The total count for each parameter for all the datasets is tabulated in Table II.

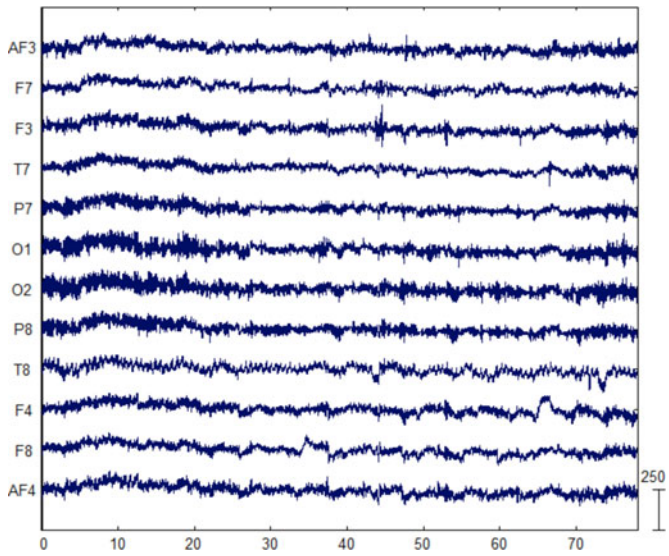

Fig. 6. 12-channel eye blink artifact-free EEG data using the proposed algorithm from Dataset 1. *X*-axis is time in seconds and *Y*-axis is amplitude in microvolts.

Average sensitivity and average specificity for the datasets are calculated with equations given below:

$$\text{Sensitivity} = \frac{\text{TP}}{\text{TP} + \text{FN}} \times 100\% \tag{11}$$

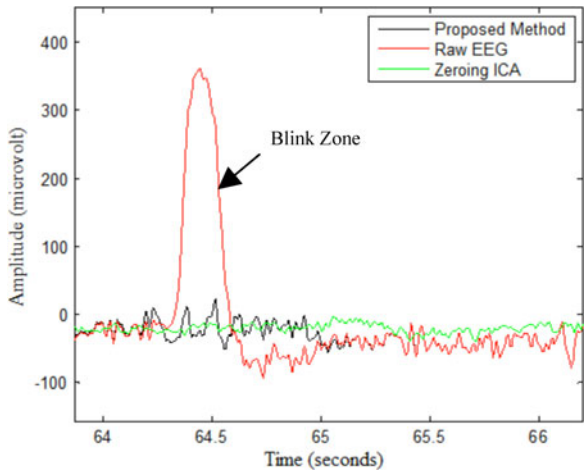

Fig. 7. Comparison of a section of the processed EEG data (AF3 frontal electrode location of Dataset 1) using the proposed method and the zeroing-ICA artifact removal method.

TABLE II
PERFORMANCE EVALUATION OF THE PROPOSED ALGORITHM FOR THE GIVEN DATASETS

True Positive (TP): 27	False Positive (FP): 1(Type I error)
False Negative (FN): 3 (Type II error)	True Negative (TN): 53

Average Sensitivity: **90%** Average Specificity: **98%**

$$\text{Specificity} = \frac{\text{TN}}{\text{TN}+\text{FP}} \times 100\%\,. \tag{12}$$

As mentioned in [32], we also calculated the agreement rate between the proposed method and the standard visual inspection check technique using (13):

$$\text{Agreement Rate} = \frac{\text{TP}+\text{TN}}{\text{TP}+\text{TN}+\text{FP}+\text{FN}}. \tag{13}$$

The concordance between the automatic identification process and the visual identification process is found to be 95.2%.

The performance of the discussed method is also evaluated using the statistical metrics—correlation coefficient and mutual information over the conventional methods: zeroing ICA and wICA. Correlation coefficient determines the correlation between the reconstructed artifact free EEG data and the raw EEG data; more positive is the coefficient value, stronger is the correlation [33]. We have used an inbuilt MATLAB function *corrcoef* to compute this parameter. As suggested in [34], we have also calculated mutual information (a nonparametric measure of relevance between the two random variables) to find how much information artifact free EEG signal "*a*" shares with the raw EEG signal "*b*". Mathematically, it is found using Kullback–Leibler divergence between the probability distribution functions as

$$MI = \int_{\infty}^{\infty}\int_{\infty}^{\infty} f(a,b)\log\frac{f(a,b)}{f(a)f(b)}dadb \tag{14}$$

TABLE III
COMPARISON WITH CONVENTIONAL METHODS

Metric	Electrode location	Proposed Method	Zeroing ICA	wICA
Correlation Coefficient	AF3	0.5613	0.3394	0.4570
	F7	0.6372	0.4448	0.4480
	F3	0.7665	0.5016	0.5713
	FC5	0.8010	0.5299	0.5633
	T7	0.7543	0.5325	0.5397
	P7	0.9701	0.7996	0.6964
	O1	0.9161	0.7648	0.7123
	O2	0.9281	0.7598	0.7046
	P8	0.8898	0.7020	0.7027
	T8	0.8543	0.7512	0.6289
	FC6	0.7571	0.5011	0.5274
	F4	0.7808	0.6250	0.6069
	F8	0.6476	0.4624	0.5129
	AF4	0.6154	0.3602	0.4731
Mutual Information	AF3	0.9058	0.1978	0.3878
	F7	0.9068	0.3458	0.3187
	F3	1.1162	0.4128	0.4142
	FC5	1.0926	0.3453	0.3410
	T7	1.2780	0.5675	0.4007
	P7	1.6578	1.1367	0.5364
	O1	1.5458	0.9426	0.5494
	O2	1.5297	0.8583	0.4893
	P8	1.5792	1.0185	0.5689
	T8	1.4447	0.8615	0.4731
	FC6	1.0245	0.2397	0.3080
	F4	1.1763	0.5308	0.3839
	F8	1.0354	0.3805	0.3907
	AF4	0.9345	0.2123	0.3595

The metrics tabulated in the table are the average values for the electrode locations across all 7 datasets. Note that each dataset consist of only best 12- channel EEG recordings out of 14-channel EPOC EEG recordings.

where $f(a, b)$ is the joint pdf and $f(a)$ and $f(b)$ are the marginal pdfs. If the mutual information[1] is larger, the resemblance of the reconstructed artifact free signal with the raw signal is closer. The average respective values of correlation coefficient (0.7771/0.5767/0.5817) and mutual information (1.231/0.5750/0.4230) for all the datasets, enumerated in Table III, demonstrate improved performance of the proposed method over conventional methods. In addition to statistical analysis, execution time of the proposed artifact removal technique is also compared with the standard wavelet ICA and is plotted in Fig. 8. The figure depicts that denoising only required artifact related components (as proposed in this study) significantly reduces mean execution time from 0.1078 s (SD = 0.004) to 0.060 s (SD = 0.021) in contrast to the conventional wICA technique. It is to be noted that the execution time for the zeroing-ICA method depends upon the how quickly and accurately an expert mark the noisy ICs for denoising.

In order to further analyze over frequency domain, magnitude squared spectral coherence measure between reconstructed artifact free data and the raw EEG data is computed (AF3 electrode location of Dataset 1) for all three methods and is plotted in Fig. 9 for comparison. Magnitude squared spectral coherence estimate between 0 and 1 indicates how well the two-signals, x and y, corresponds at various frequencies. It is a function of

[1]We have used open source MATLAB function *minfo.m* developed by Dr. Jason Palmer; [Online]. Available at: http://sccn.ucsd.edu/~jason/minfo.m.

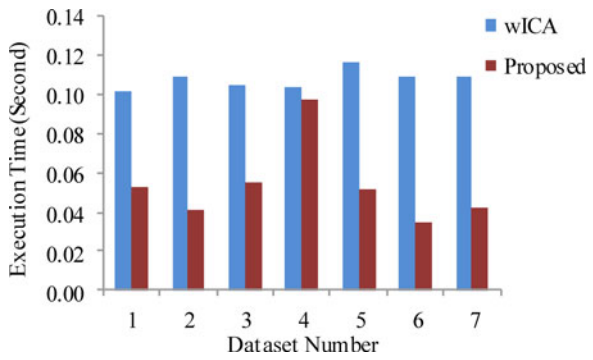

Fig. 8. Time elapsed (in seconds) for the execution of proposed method and conventional wICA artifact removal method for all datasets.

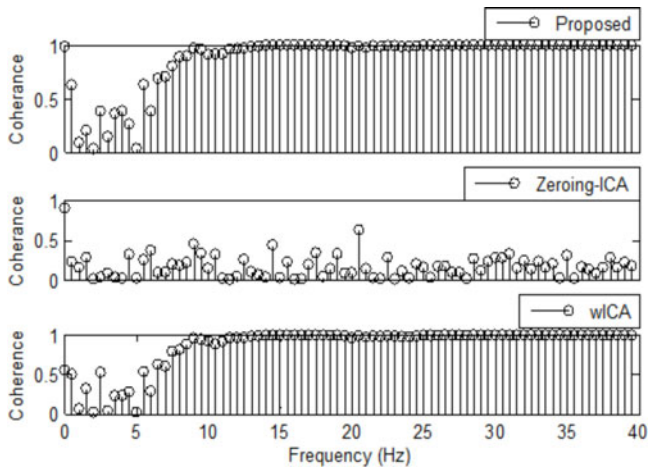

Fig. 9. Magnitude squared coherence measure plot for Dataset 1 (AF3 location) with the proposed method and other conventional techniques.

power spectral density of two signals (x: Raw EEG data, and y: Reconstructed artifact-free EEG data) and is mathematically computed as

$$\mathrm{C_{xy}(f)} = \frac{P_{\mathrm{xy}}(f)^2}{P_{\mathrm{xx}}(f)P_{\mathrm{yy}}(f)} \tag{15}$$

where $P_{\mathrm{xy}}(f)$ is the cross power spectral densities of signal, $P_{\mathrm{xx}}(f)$ is power spectral density of raw EEG signal, and $P_{\mathrm{yy}}(f)$ is power spectral density of artifact-free EEG signal. Power spectral densities are calculated over FFT length of 256 with 50% overlapped Hamming window using MATLAB *mscohere* function. Fig. 9 shows that the coherence between signals is strongest for frequencies above 10 Hz with the proposed method in comparison to other methods.

V. Discussion

We envision that wearable ambulatory EEG systems in future will be minimalistic and pervasive beyond clinical settings. There is copious research on artifact removal in higher density EEG systems [1], [12], [18], [34]; the challenge still lies when we have small number of channels. This study explores a fully automatic and computationally fast algorithm to remove eye-blink artifacts from an EEG system with few channels.

Extended-Infomax ICA decomposition employed in this study is used for 12 channels, but is effective on large number of EEG channels as well [35], [36]. Eye blinks are typically found to dominate 2–3 channels in high-dimension EEG data, so we speculate that our method can be used for dense EEG systems; however, it needs to be experimentally tested. It should be noted that for EEG systems, the quality of ICA relies on preprocessing (e.g., dimensional reduction in dense EEG) and sufficient number of time points used for decomposition [37].

For identification of eye blink artifact related ICs, we have used two-pronged approach by using two conservative thresholds so as to minimize type I and type II error. The first threshold: lower limit of 95% CI of mean for mMSE identify ICs on the basis of data regularity, while the second threshold: upper limit of 95% CI of mean for Kurtosis detect ICs on the basis of their shape of probability distribution. For the given datasets, 95% CI threshold limits were found to be the most robust limits in order to identify blink ICs in comparison with 90% CI and 98% CI limits. As a result, with the given thresholds, we expect least type 1 and type II error. However, to account for peculiarities of other artifacts (e.g., muscle movement, cardiac activities), the algorithm can be modified to different threshold strategies.

This study employs mMSE for a typical artifactual activity, i.e., eye-blink detection as it provides information regarding the regularity of EEG data, however it might be useful for identifying rhythmic cardiac activities in EEG.

For wavelet decomposition, we also compared biorthogonal wavelet with fast, orthogonal Haar wavelet which resulted in better overall reconstruction [correlation coefficient (0.8223/0.6573/0.6737) and mutual information (1.609/0.7670/0.7910)]. However, biorthogonal wavelet has shown much better reconstruction specifically over the blinking zone (see Fig. 7).

VI. Conclusions

This paper presents a new unsupervised, fast algorithm for fully automatic identification and suppression of the eye blink related ICs by using mMSE and Kurtosis as markers and wavelet decomposition as denoising tool. mMSE fetches the regularity information from the ICs over multiple temporal scales and can efficiently identify the ICs with eye blink characteristics. Kurtosis enhances the performance by identifying the ICs with super-Gaussian 'peaked' probability distributions, which imitates the eye blink distributions. Using lower and upper bounds of 95% CI for the mean as threshold, the blink related artifactual ICs identified (jointly by the markers) are then denoised using DWT with Biorthogonal wavelet as the basis function. The statistical metrics: Sensitivity (90%), Specificity (98%) demonstrates that the proposed method can denoise the eye blink artifacts effectively. The method offers the advantage of neither requiring manual intervention for IC identification nor additional EOG channel for reference. The results in terms of mutual information, correlation coefficient, and spectral coherence also show better EEG signal reconstruction (with neural activity related

ICs intact) over the commonly used zeroing-ICA and wICA methods. The algorithm discussed in this paper is intended for eye blink correction, but can be applied to other ocular artifacts, i.e., saccades and fixations and even cardiac artifacts with minor modifications in thresholds. To confirm our hypothesis that our method will work in higher dimensions, we need to apply our method to a higher dimension EEG system.

ACKNOWLEDGMENT

The authors are grateful to Dr. J. Jennings (Department of Biomedical Engineering, University of Memphis) for providing assistance in statistical interpretation of the results. The authors would like to thank the anonymous reviewers and editors for their valuable comments, suggestions, and insights to improve the quality of this manuscript.

REFERENCES

[1] D. Hagemann and E. Naumann, "The effects of ocular artifacts on (lateralized) broadband power in the EEG," *Clin. Neurophysiol.*, vol. 112, no. 2, pp. 215–231, 2001.

[2] J. C. Woestenburg, M. N. Verbaten, and J. L. Slangen, "The removal of the eye-movement artifact from the EEG by regression analysis in the frequency domain," *Biol. Psychol.*, vol. 16, pp. 127–147, 1983.

[3] M. T. Akhtar, W. Mitsuhashi, and C. J. James, "Employing spatially constrained ICA and wavelet denoising, for automatic removal of artifacts from multichannel EEG data," *Signal Process.*, vol. 92, no. 2, pp. 401–416, 2012.

[4] J. Gotman, D. R. Skuce, C. J. Thompson, P. Gloor, J. R. Ives, and F. W. Ray, "Clinical applications of spectral analysis and extraction of features from electroencephalograms with slow waves in adult patients," *Electroencephalogr. Clin. Neurophysiol.*, vol. 35, pp. 225–35, 1973.

[5] N. A. de Beer, M. van de Velde, and P. J. Cluitmans, "Clinical evaluation of a method for automatic detection and removal of artifacts in auditory evoked potential monitoring," *J. Clin. Monit.*, vol. 11, pp. 381–91, 1995.

[6] T. P Jung, S. Makeig, M. Westerfield, J. Townsend, E. Courchesne, and T. J. Sejnowski, "Analysis and visualization of single-trial event-related potentials," *Hum. Brain Mapp*, vol. 14, pp. 166–85, 2001.

[7] T. D. Lagerlund, F. W. Sharbrough, and N. E. Busacker, "Spatial filtering of multichannel electroencephalographic recordings through principal component analysis by singular value decomposition," *J. Clin. Neurophysiol.*, vol. 14, pp. 73–82, 1997.

[8] S. V. Ramanan, N. V. Kalpakam, and J. S. Sahambi, "A novel wavelet based technique for detection and de-noising of ocular artifact in normal and epileptic electroencephalogram," in *Proc. Int. Conf. Commun. Circuits Syst.*, 2004, vol. 2, pp. 1027–31.

[9] V. Krishnaveni, S. Jayaraman, S. Aravind, V. Hariharasudhan, and K. Ramadoss, "Automatic identification and removal of ocular artifacts from EEG using wavelet transform," *Meas. Sci. Rev.*, vol. 6, no. 4, pp. 45–57, 2006.

[10] P. S. Kumar, R. Arumuganathan, K. Sivakumar, and C. Vimal, "Removal of ocular artifacts in the EEG through wavelet transform without using an EOG reference channel," *Int. J. Open Problems Comput. Math.*, vol. 1, no. 3, pp. 188–200, 2008.

[11] G. Hosna and A. Erfanian, "A fully automatic ocular artifact suppression from EEG data using higher order statistics: Improved performance by wavelet analysis," *Med. Eng. Phys.*, vol. 32, no. 7, pp. 720–729, 2010.

[12] A. Delorme, T. Sejnowski, and S. Makeig, "Enhanced detection of artifacts in EEG data using higher-order statistics and independent component analysis," *Neuroimage*, vol. 34, no. 4, pp. 1443–1449, 2007.

[13] R. Mahajan and B. I. Morshed, "Sample entropy enhanced wavelet-ICA denoising technique for eye blink artifact removal from scalp EEG dataset," in *Proc. 6th Int. IEEE/EMBS Conf. Neural Eng.*, 2013, pp. 1394–1397.

[14] D. B Keith, C. C. Hoge, R. M. Frank, and A. D. Malony, "Parallel ICA methods for EEG neuroimaging," in *Proc. 20th Int. Parallel Distrib. Process. Symp.*, 2006, pp. 25–29.

[15] E. Kroupi, A. Yazdani, J. M. Vesin, and T. Ebrahimi, "Ocular artifact removal from EEG: A comparison of subspace projection and adaptive filtering methods," in *Proc. 19th Eur. Signal Process. Conf.*, Barcelona, Spain, 2011, pp. 1355–1359.

[16] A. Hyvarinen and E. Oja, "Independent component analysis: Algorithms and applications," *Neural Netw.*, vol. 13, no. 4–5, pp. 411–430, 2000.

[17] A. J. Bell and T. J. Sejnowski, "An information maximization approach to blind separation and blind deconvolution," *Neural Comput.*, vol. 7, pp. 1129–1159, 1995.

[18] A. Greco, N. Mammone, F. C. Morabito, and M. Versaci, "Semi-automatic artifact rejection procedure based on Kurtosis, Renyi's entropy and independent component scalp maps," in *Proc. Int. Enformatika Conf.*, 2005, pp. 22–26.

[19] W. Bosl, A. Tierney, H. T. Flusberg, and C. Nelson, "EEG complexity as a biomarker for autism spectrum disorder risk," *BMC Med.*, vol. 9, no. 1, pp. 1–16, 2011.

[20] M. Costa, A. L Goldberger, and C. K. Peng, "Multiscale entropy analysis of biological signals," *Phys. Rev. E*, vol. 71, no. 2, p. 021906, 2005.

[21] H. B. Xie, W. X. He, and H. Liu, "Measuring time series regularity using nonlinear similarity-based sample entropy," *Phys. Lett. A*, vol. 372, no. 48, pp. 7140–7146, 2008.

[22] G. Barbati, C. Porcaro, F. Zappasodi, P. M. Rossini, and F. Tecchio, "Optimization of an independent component analysis approach for artifact identification and removal in magnetoencephalographic signals," *Clin. Neurophysiol.*, vol. 115, no. 5, pp. 1220–1232, 2004.

[23] N. P. Castellanos and V. A. Makarov, "Recovering EEG brain signals: artifact suppression with wavelet enhanced independent component analysis," *J. Neurosci. Methods*, vol. 158, pp. 300–312, 2006.

[24] V. J. Samar, A. Bopardikar, R. Rao, and K. Swartz, "Wavelet analysis of neuroelectric waveforms: A conceptual tutorial," *Brain Language*, vol. 66, pp. 7–60, 1999.

[25] H. T. Gorji, H. Taheri, A. Koohpayezadeh, and J. Haddadnia, "Ocular artifact detection and removing from EEG by wavelet families: A comparative study," *J. Inf. Eng. Appl.*, vol. 3, no. 13, pp. 39–47, 2013.

[26] H. Ghandeharion and A. Erfanian, "A fully automatic ocular artifact suppression from EEG data using higher order statistics: improved performance by wavelet analysis," *Med. Eng. Phys.*, vol. 32, no. 7, pp. 720–729, 2010.

[27] D. L. Donoho and I. M. Johnstone, "Ideal spatial adaptation by wavelet shrinkage," *Biometrika*, vol. 81, no. 3, pp. 425–455, 1994.

[28] B. S. Raghavendra and D. N. Dutt, "Wavelet enhanced CCA for minimization of ocular and muscle artifacts in EEG," *World Academy Sci. Eng. Technol.*, vol. 57, pp. 1027–1032, 2011.

[29] M. Mamun, M. Al-Kadi, and M. Marufuzzaman, "Effectiveness of wavelet denoising on electroencephalogram signals," *J. Appl. Res. Technol.*, vol. 11, no. 1, pp. 156–160, 2013.

[30] I. M. Johnstone and B. W. Silverman, "Wavelet threshold estimators for data with correlated noise," *J. R. Statistical Soc.: Series B (Statistical Methodology)*, vol. 59, no. 2, pp. 319–351, 1997.

[31] A. Delorme, H. Serby, and S. Makeig. Independent component analysis of EEG data. (2014, Jan.). [Online]. Online. Available: http://sccn.ucsd.edu/eeglab/maintut/ICA_decomposition.html.

[32] S. Devuyst, T. Dutoit, T. Ravet, P. Stenuit, M. Kerkhofs, and E. Stanus, "Automatic processing of EEG-EOG-EMG artifacts in sleep stage classification," in *Proc. 13th Int. Conf. Biomed. Eng.*, 2009, vol. 23, pp. 146–150.

[33] M. Zima, P. Tichavsky, K. Paul, and V. Krajca, "Robust removal of short-duration artifacts in long neonatal EEG recordings using wavelet-enhanced ICA and adaptive combining of tentative reconstructions," *Physiol. Meas.*, vol. 33, no. 8, pp. N39–N49, 2012.

[34] J. W. Kelly, D. P. Siewiorek, A. Smailagic, J. L. Collinger, D.J. Weber, and W. Wang, "Fully automated reduction of ocular artifacts in high-dimensional neural data," *IEEE Trans. Biomed. Eng.*, vol. 58, no. 3, pp. 598–606, Mar. 2011.

[35] T. W. Lee, M. Girolami, and T. J. Sejnowski, "Independent component analysis using an Extended Infomax algorithm for mixed subgaussian and supergaussian sources," *Neural Comput.*, vol. 11, no. 2, pp. 417–441, 1999.

[36] J. Onton and S. Makeig. "Information-based modeling of event-related brain dynamics," *Progress Brain Res.*, vol. 159, pp. 99–120, 2006.

[37] S. Makeig, T-P. Jung, A. J. Bell, D. Ghahremandi, and T. J. Sejnowski, "Blind separation of auditory event-related brain responses into independent components," in *Proc. Nat. Acad. Sci.*, 1997, vol. 94, no. 20, pp. 10979–84.

Authors' photographs and biographies not available at the time of publication.